PHYSICAL PROPERTIES OF HIGH-T_c SUPERCONDUCTORS

High critical temperatures are not the only interesting property of cuprate superconductors. An accumulation of consistent experimental results hints at the unusual nature of the metallic state above T_c.

Bertram Batlogg

Four years of intensive research following J. Georg Bednorz and K. Alex Müller's discovery[1] of high-temperature superconductors has produced about 18 000 publications. An overview of all physical properties is thus beyond the scope of this article,[2] so I will focus on a few topics that are widely perceived to hold the key to understanding these fascinating compounds.

Aside from the high T_c, the superconducting state of the cuprates so far has turned out to be less remarkable than the "normal" metallic state that occurs at temperatures above T_c. Currently much work is focused on whether the metallic cuprates are like ordinary metals such as aluminum or lead, and on those unusual properties that are unique attributes of the metallic cuprates. The dynamics of charge and spin degrees of freedom are of particular interest because these metals are derived from insulating antiferromagnets through the removal or addition of electrons.

Progress toward understanding these materials is closely tied to the quality of experimental data, which in turn depends on sample quality. The growth of sizable crystals (see figure 1) is hampered by the chemical complexity of the cuprates (see also Arthur W. Sleight's article on page 24). And yet, high quality crystals are a prerequisite to achieve quantitative and reproducible results, particularly because the anisotropy of the cuprates requires that measurements be done along different axes of the crystals.

Essential building blocks

The structure of the cuprate superconductors can be viewed as stacks of closely spaced CuO_2 layers, separated by charge reservoir building blocks[3] (see James D. Jorgensen's article on page 34). Since the CuO_2 layers have been recognized as the essential part for superconductivity, a quite useful approach to studying superconductivity is to modify the charge carrier concentration in the active CuO_2 layers through chemical modification of the adjacent charge reservoirs. Examples of such changes[4] include the addition or removal of oxygen or substitution of some metal ions with heterovalent ions, such as Ba^{2+} for La^{3+} in La_2CuO_4 or "Ce^{4+}" for Nd^{3+} in Nd_2CuO_4. Ba acts as a dopant of holes, while Ce is a dopant of electrons. For any given compound family, the superconducting transition temperature is maximized in a narrow range of hole (or electron) concentration, typically around 0.15–0.2 holes per CuO_2. The maximum T_c's range from 38 K in $La_{2-x}Sr_xCuO_4$ to near 125 K in $Tl_2Ba_2Ca_2Cu_3O_{10}$.

Figure 2 shows a generic phase diagram for cuprates, illustrating how magnetic and transport properties vary as the hole concentration is changed. Starting with an insulating, long-range ordered antiferromagnet, the ordering temperature (Néel temperature) drops rapidly when the carrier concentration per CuO_2 is changed by about 0.01–0.02. Metallic transport and superconductivity both appear when the electron concentration deviates from the undoped phase by approximately 0.1 per CuO_2. We note the absence in this range of a normal metal phase as T approaches zero—that is, the compounds are either superconducting or insulating at low doping levels. On the right of the superconducting range, the materials are metallic but not superconducting, and their properties resemble those of ordinary metals. To simplify the discussion of the metallic state, I will concentrate on the hole-doped cuprates and on those compositions that exhibit the highest T_c's within their compound families. It turns out that the physical properties of the optimized compositions

Bertram Batlogg is head of the Solid State and Physics of Materials Research Department at AT&T Bell Laboratories, Murray Hill, New Jersey.

RUTHERFORD APPLETON LABORATORY, UK

Large La_2CuO_4 crystals (the antiferromagnetic parent compound of a family of cuprate superconductors) mounted on a goniometer for inelastic neutron-scattering studies of spin excitations. These plate-like crystals are grown by Sang-Wook Cheong (AT&T Bell Laboratories) and Zachary Fisk (Los Alamos National Laboratory) using CuO_2 as a solvent (flux technique). The in-plane size reaches up to 8–10 cm. **Figure 1**

are very similar despite T_c's that differ by as much as a factor of five.

Electronic states and Fermi surface

An initial question concerns the nature of the electronic states near the Fermi energy E_F, which are responsible for the transport properties. Bonding between nominal Cu^{2+} and O^{2-} has both ionic and covalent character and involves the Cu $3d$ and O $2p$ orbitals. The origin of the covalency is ultimately rooted in the proximity in energy of the $3d$ and $2p$ levels, and thus it is specific to the combination of these two elements. (A similar energy degeneracy occurs between the $6s$ levels of Pb and Bi and the $2p$ level of O in the $BaBi_{1-x}Pb_xO_3$ superconductors.) Various types of electron spectroscopies confirm this covalent mixing and reveal that the highest occupied electronic states—the ones near E_F—have both $3d$ and $2p$ character, with a predominance of the latter. Consequently the holes introduced in the CuO_2 layers by doping are not located only at the Cu sites or only at the O sites, but have a mixed character.

More important is the question of the existence of a Fermi surface and its shape. The Fermi surface is the locus in momentum space where the occupation of the electronic states drops abruptly and where the energy required to create particle–hole excitations vanishes. In a simple metal, with a spherical Fermi surface, at $T = 0$ all states with momentum k less than the Fermi momentum k_F are filled, and states with $k > k_F$ (and hence energy $E > E_F$) are empty. In general, the shape of the Fermi surface is determined by the momentum dependence of electronic energies $E(\mathbf{k})$, also called electronic band structure. $E(\mathbf{k})$ is material specific, and great advances have been made in calculating $E(\mathbf{k})$ even for complicated compounds such as the cuprates. When one considers the strong correlations among the electrons in the cuprates, the existence of a Fermi surface is not obvious.

Photoemission electron spectroscopy is one of the experimental tools used to study $E(\mathbf{k})$. The emission intensity is measured as a function of energy and emission angle along the principal symmetry directions of the crystal. The best results available are for $Bi_2Sr_2CaCu_2O_8$, for which cleaving in a vacuum produces clean and chemically stable surfaces.[5] The main result is that the measured energy bands $E(\mathbf{k})$ cross the Fermi energy at points in $\mathbf{k}$ space that are given by the calculations, confirming the presence of a Fermi surface. In addition, more subtle but important details of the emission spectra,

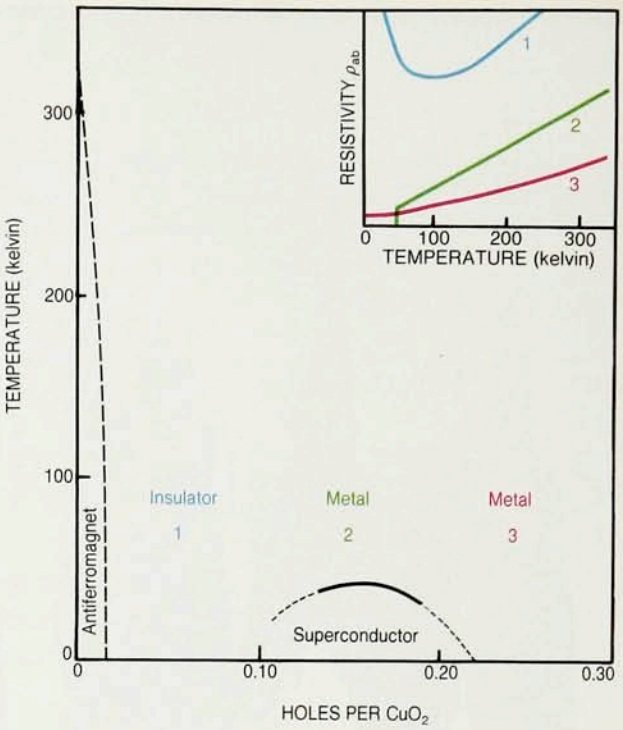

Generic phase diagram for layered cuprates. As the electron concentration in the CuO_2 layers is changed by doping the parent compound, a transition occurs from an insulating antiferromagnet with long-range magnetic order to (1) an insulator with only short-range magnetic order (and a spin-glass ground state), to (2) a metal with a superconducting ground state, and finally to (3) a normal metal. This generic phase diagram has not yet been mapped out quantitatively for all structural families of cuprates, since it is not always possible to change the chemical composition over a wide enough range. Inset shows in-plane resistivity behavior for three different doping levels. **Figure 2**

such as peak shape and background intensity, can be analyzed to decide if a conventional Fermi-liquid description is appropriate. Despite great technical progress in the last few years, the experimental resolution is not quite sufficient to give an unambiguous answer. There is some agreement, nevertheless, that the spectra are suggestive of an unconventional Fermi liquid. One signature of this is a lifetime broadening of the electronic states at energy E that grows like $|E - E_F|^n$, with the best value of n being approximately 1 (in ordinary Landau Fermi liquids, n is equal to or greater than 2).

Measurements of specific heat and spin susceptibility probe the density of electronic states in an energy window around E_F of several times $k_B T$, where k_B is Boltzmann's constant. The experimental density of states is within a factor of 2 of what one gets from the band structure calculations, and therefore it indicates only a modest increase in the density of states due to interaction with, for example, phonons.

Charge dynamics: Transport above T_c

As one might expect from the crystal structure, the electrical properties of the layered cuprates are highly anisotropic. The electrical resistivity of $Bi_2Sr_2CaCu_2O_8$, for example, can be up to 10^5 times larger in the c direction (perpendicular to the CuO_2 layers) than it is in the a and b directions (along the layers). The degree of anisotropy is specific to a compound family and reflects how effectively the charge reservoir layers block the coherent motion of electrons between the CuO_2 layers. The resistivities parallel and perpendicular to the planes are also different in character. The in-plane resistivity ρ_{ab} behaves like that of a metal, increasing as the temperature is raised, while the perpendicular resistivity ρ_c is reminiscent of semiconductor behavior, decreasing upon heating. (A possible exception is found in $YBa_2Cu_3O_7$, which is the least anisotropic material; in some crystals of $YBa_2Cu_3O_7$ ρ_c has a metallic character, although it is still more than 10 times larger than ρ_{ab}.) The semiconductor-like $\rho_c(T)$ can be several orders of magnitude greater than the maximum metallic value.

Figure 3a shows $\rho_{ab}(T)$ for several selected crystals. A few aspects are worth pointing out: The resistivities are all close in magnitude; they increase approximately linearly with temperature over wide temperature ranges; and they are quite small when extrapolated to zero temperature.[6] The striking similarity of the $\rho(T)$ curves for optimized compositions is evidence that the common CuO_2 layers are the electronically active building blocks in otherwise very different crystal structures. The mean-free path at 100 K is estimated to be 100–200 Å for $YBa_2Cu_3O_7$, which is long compared to the lattice parameter of 3.8 Å. The electrons are thus only weakly scattered, and these metals are considered "clean." Furthermore, the slopes $d\rho/dT$ fall in a narrow range near 0.5 $\mu\Omega$ cm/K.

The unusual character of the charge dynamics of the cuprates is best seen by going beyond the temperature dependence of the dc conductivity $\sigma_0(T) \equiv 1/\rho_{ab}(T)$ to the optically measured frequency-dependent $\sigma(\omega,T)$ (see figure 4a).[7] At first sight the low frequency parts of the rapidly decreasing $\sigma(\omega)$ curves are reminiscent of charge carriers being scattered at a frequency-independent rate of $1/\tau_0$, which increases with temperature, as observed in simple metals. However, the simplest scattering form of this constant-τ_0 model—a Lorentzian with a width $\hbar/\tau_0$ of approximately $k_B T$—deviates significantly from the measured $\sigma(\omega)$ curves. A consistent description of the observed $\sigma(\omega)$, within a model of carriers scattering from excitations (such as phonons), requires that the scattering rate depend on both temperature and frequency. The peculiarity of the cuprate charge dynamics is reflected in the form of this rate: $\hbar/\tau^*(\omega,T)$ is given by the greater of $k_B T$ or $\hbar\omega$. (A proposed functional form is $(\hbar/\tau^*)^2 = (\alpha k_B T)^2 + (\beta\hbar\omega)^2$, with α and β of order unity.) These results imply that the charge carriers interact with an excitation spectrum that extends over a broad energy range well beyond phonon frequencies. Furthermore the enhanced conductivity in the range of several tens of eV may suggest the existence of additional electronic excitations between different bands.

Raman scattering reveals the existence of electronic excitations that may be closely linked to the scattering that leads to $\sigma(\omega,T)$. Contrary to our experience with conventional metals, where light is scattered by particle–hole excitations up to frequencies of order 50 cm^{-1}, a broad continuum of electronic excitations is observed in the metallic cuprates. The important features of the imaginary part of the Raman response function R″ are shown[8] in figure 4b. It remains to be determined whether the broad Raman scattering, which is highly characteristic of the cuprates, is due to spin or charge excitations or both. An important conclusion from the transport and light-scattering experiments is that there is no scale for

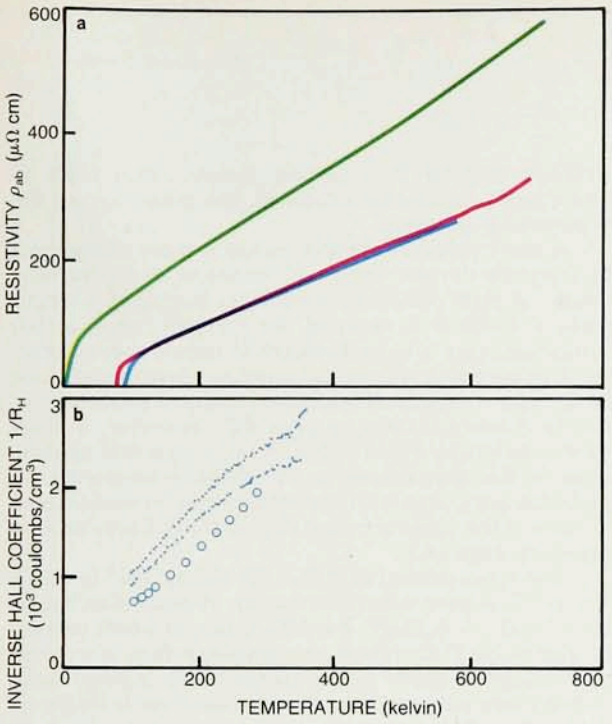

Resistivity and Hall coefficient in crystals of different cuprates. **a:** The resistivity ρ_{ab} along the CuO_2 planes is similar for the various compounds and depends nearly linearly on temperature over a wide temperature range. For optimized compounds the behavior is almost identical. The blue and red curves are optimized compounds ($YBa_2Cu_3O_7$ and $Bi_2Sr_{2.2}Ca_{0.8}Cu_2O_8$, respectively). The green curve is $Bi_{2.1}Sr_{1.9}CuO_6$. **b:** The inverse of the Hall coefficient, shown here for measurements using three different $YBa_2Cu_3O_7$ single crystals, exhibits strong temperature dependence over the entire range of measurement. (Adapted from refs. 6, 10.)
Figure 3

low-energy excitations other than the temperature itself.[9]

Closely related to the resistivity is the Hall effect, a measure of the off-diagonal elements of the conductivity tensor. In a simple metal, the Hall effect is a measure of the carrier concentration and is only weakly temperature dependent. The reciprocal of the Hall coefficient, $1/R_H$, is shown in figure 3b for $YBa_2Cu_3O_7$ single crystals.[10] Studies of this and other optimized superconductors suggest that the observed strong temperature dependence is an intrinsic property of the cuprates. Strong temperature dependence of the Hall effect is observed in ordinary metals only at temperatures below a fraction (a fifth to a half) of the Debye temperature θ_D, which is the characteristic energy scale for phonons. In the so-called 1-2-3 compounds, θ_D is 400–450 K, which makes it unlikely that the observed strong temperature dependence is caused by electron–phonon scattering. Invoking more than one type of carrier (such as heavy and light electrons or holes and electrons described by different bands) to explain $\rho(T)$ and $R_H(T)$ would require a fortuitous and unlikely combination of temperature-dependent carrier concentrations and mobilities.

Magnetic properties

The undoped parent compounds of the superconducting cuprates are magnetic insulators whose magnetic properties are well understood now. The magnetic moments of the nearly filled Cu^{2+} $3d^9$ shell form a spin-$\frac{1}{2}$ Heisenberg system on a two-dimensional square lattice. Strong antiferromagnetic super exchange J provides the dominant interaction between neighboring Cu sites ($J \sim 10$–130 meV). A weak interlayer coupling leads to long-range three-dimensional antiferromagnetic ordering,[11] at a temperature much lower than the in-plane exchange energy. La_2CuO_4, with a Néel temperature of about 330 K, has been thoroughly investigated in search of expected quantum effects. However, one finds that both the static susceptibility and spin excitations are well described by a classical model. Quantum effects introduce small modifications of the numerical parameters, but they don't lead to quantum frustration or other qualitatively new dynamics.

A gradual change of the magnetic response is observed upon the introduction of carriers. The static susceptibility is only weakly temperature dependent between T_c and 400 K for optimized superconductors, and it increases systematically with the number of closely spaced CuO_2 layers, each layer contributing 1.2–1.5×10^{-3} emu/mole to the spin susceptibility.

On a local scale, nuclear magnetic resonance and nuclear quadrupole resonance are used to investigate the spin dynamics, since the nuclear moments are coupled to the electron's spin degree of freedom and probe the low-frequency limit of the magnetic susceptibility.[12] The nmr Knight shift, which in essence is a local susceptibility probe, exhibits the same temperature dependence at the Cu and the O sites, and both closely follow the static, macroscopically measured susceptibility. Thus a single-species spin-system description seems appropriate.

A different aspect of spin dynamics can be examined by the nuclear-moment relaxation rate. The experiments reveal distinctly different magnitudes and temperature dependence for the Cu and O nuclear relaxation rates. This difference is another characteristic of the cuprate metallic state, and it has been interpreted as being due to a wavevector ($\mathbf{q}$) dependence of the generalized magnetic susceptibility $\chi(\mathbf{q},\omega\rightarrow0)$. Because of the geometric arrangement of the Cu and O atoms, one concludes from these nmr results that $\chi(\mathbf{q},\omega\rightarrow0)$ is enhanced near the Brillouin zone corner, $\mathbf{q}=(\pi/a_0,\pi/a_0)$, where a_0 is the lattice parameter. This enhancement, when interpreted as evidence for strong antiferromagnetic correlations among the spins, is an essential ingredient in some theoretical approaches to high-T_c superconductivity. Conclusive neutron scattering results, which could support this interpretation, are not yet available for optimized $YBa_2Cu_3O_7$ because it is difficult to grow crystals that are large enough and of the correct composition.

The spin dynamics is markedly different in superconductors with reduced T_c and compositions closer to the antiferromagnetic limit (see figure 2) than in those with optimized T_c. The static susceptibility χ, nmr Knight shift and also the nuclear relaxation rates decrease upon cooling below room temperature. It has been suggested that these reductions indicate a suppression of low-frequency spin excitations due to the formation of a pseudogap in the excitation spectrum, reminiscent of the spin gaps in linear chains of $S=1$ antiferromagnets.

We have considered a range of properties: the broadening of the electronic states; the characteristic temperature and frequency dependence of the charge-carrier relaxation time deduced from electrical conductivity measurements; the broad electronic excitation spectrum revealed by Raman spectroscopy; and the difference between Cu and O nuclear relaxation rates. These are

widely seen to be the fingerprints of the electronic states peculiar to the optimized two-dimensional metallic cuprates.

The superconducting state

It became clear in the first few months after its discovery that cuprate superconductivity involves the pairing of quasiparticles (electrons), as expressed in an effective charge of $e^* = 2e$. The experiments included observation of the ac-Josephson effect, flux jump measurements, direct measurements of the magnetic flux quantum ϕ_0 and Little–Parks oscillations. Andreev scattering revealed that the pairs are made up of electrons with opposite momentum. Various aspects of the superconducting state are of interest, especially the identification of the excitations that mediate the pairing, the energy gap $\Delta(\mathbf{k},T)$, the coherence length ξ and the magnetic penetration depth λ.

The pronounced layered structures of the cuprates influence electronic properties not only in the normal, but also in the superconducting state. In some respects, these compounds act as an assembly of weakly coupled superconducting sheets. The values for ξ and λ are known both parallel and perpendicular to the CuO_2 planes and are consistently deduced from a variety of measurements. The most complete data set available is for $YBa_2Cu_3O_7$, which is also one of the least anisotropic materials. In the low-temperature limit, one finds $\xi_{ab} = 14 \pm 2$ Å, $\xi_c = 1.5$–3 Å, $\lambda_{ab} = 1400$ Å and $\lambda_c \sim 7000$ Å.

For comparison, the values for niobium are $\lambda \cong 350$ Å and $\xi \cong 400$ Å. The length scales in the cuprates are rather extreme, and they result from material-specific properties. Cuprate superconductors are of extreme type II ($\lambda/\xi \gg 1$) and are in the "clean" limit—that is, $\ell(T=0)$ is much shorter than the electron's mean-free path (100–200 Å) near T_c.

An external magnetic field can penetrate the cuprates to a relatively large depth (λ) because the few carriers (concentration $2\text{–}5 \times 10^{21}$ cm^{-3}) are not effective in shielding the field. The very short coherence length ξ, which is a measure of the spatial extent of a superconducting pair, results from a different set of materials properties. Within BCS pairing theory, $\xi_0 = \hbar v_F / \pi \Delta(0)$, where v_F is the Fermi velocity and $\Delta(0)$ is the superconducting-gap parameter, which is proportional to T_c. A ξ_0 of 15 Å is indeed consistent with $v_F = 1.1 \times 10^7$ cm/sec and $2\Delta(0) = 6k_BT_c$, which are typical parameters for 1-2-3 compounds. Since the coherence length ξ_c perpendicular to the CuO_2 planes is only a few angstroms, the superconducting layers are only weakly coupled when the charge reservoirs are as thick as the BiO double layers.

This superconducting anisotropy is of great practical consequence because it tends to influence the current-carrying capacity in an unfavorable way, but it also allows for the occurrence of novel physical phenomena associated with the dynamics of flux lines. (An external magnetic field penetrates a superconductor not uniformly, but along flux lines that each carry one flux quantum ϕ_0.)

The short coherence length is interesting conceptually and practically. Given the low electron concentration of less than 1 per CuO_2 and a coherence volume that includes only 5–10 CuO_2 units, one finds fewer than five pairs within one coherence volume. This is several orders of magnitude fewer than in a conventional superconductor such as aluminum, which has more than 10^4 pairs and is well-described by BCS pairing theory. This leads to pronounced fluctuation effects at the transition to the superconducting state.

A short coherence length makes it more challenging to fabricate devices based on tunneling and proximity effects. A tight control over material quality on a length scale of 10–50 Å is required, for instance, when a thin insulating layer is to be deposited to form a superconductor–insulator–superconductor junction—traditionally one of the key elements of superconducting electronics (see Randy Simon's article on page 64). However, a short coherence length would be beneficial in high-field applications at low temperatures. (At elevated temperatures, problems associated with flux motion may be encountered in some of the cuprate materials; see David Larbelestier's article on page 74.)

The upper critical field H_{c2}, the highest field in which a type II superconductor remains superconducting, is given by $H_{c2} = \phi_0 / 2\pi\xi^2$. For $YBa_2Cu_3O_7$ in a field perpendicular to the CuO_2 layers, this corresponds to more than one megagauss at low temperatures, which is about three to five times stronger than the strongest static magnetic fields achievable at present. It will be a major challenge to exploit the full range of these intrinsic limits.

Superconducting gap and superfluid density

In the superconducting state a minimum energy 2Δ, the gap energy, is required to break up a superconducting (Cooper) pair. No electronic excitations are possible below the gap. In conventional superconductors, Δ is isotropic; it is roughly the same everywhere on the Fermi surface. In superfluid ^{3}He and also in the novel class of metals known as the heavy fermion superconductors (including $CeCu_2Si_2$, UPt_3 and UBe_{13}), the gap vanishes along lines or at points on the Fermi surface. In ^{3}He, and probably also in the heavy fermion superconductors, pairing is mediated by magnetic excitations, not by phonons. Thus, it is of interest to know $\Delta(\mathbf{k},T)$ in the cuprates.

A variety of measurements indicates that a true gap exists everywhere on the Fermi surface—that is, $\Delta(\mathbf{k}) \neq 0$ for all values of $\mathbf{k}$. This conclusion is based on the variation with T of the superfluid density ρ_s at low temperatures. (Also called the order parameter, ρ_s can be thought of as the fraction of carriers condensed into the superfluid ground state.) In a conventional superconductor such as aluminum, ρ_s is constant as T approaches zero and decreases with increasing temperature as $\exp(2\Delta/k_BT)$ because of thermal excitation of pairs across the gap. In contrast, when $\Delta(\mathbf{k})$ vanishes at points or lines, there is no true gap but the density of states grows linearly or quadratically with E. Consequently, the variation of ρ_s with increasing T follows a power law that can be distinguished experimentally from the exponential variation.

In figure 5a representative results of different measurements[13] related to $\rho_s(T)$ are compared for $YBa_2Cu_3O_7$. The flatness of the curve at low T clearly indicates the existence of a non-zero gap for pair breaking over the entire Fermi surface. On cooling below T_c the superfluid density increases more rapidly than in the weak-coupling BCS limit, in agreement with the measured electronic specific-heat anomaly of 3.5–4 at T_c, which is significantly larger than the BCS anomaly of 1.43. The electronic spin susceptibility for T approaching zero also indicates the

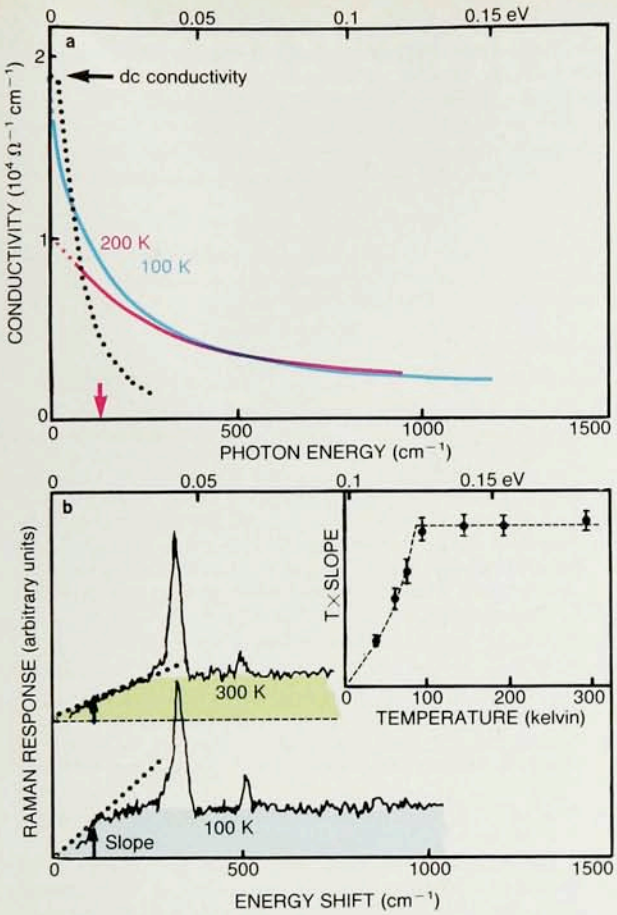

Characteristic charge dynamics in $YBa_2Cu_3O_7$ in the metallic state above $T_c = 92$ K. **a:** The frequency- and temperature-dependent conductivity $\sigma(\omega,T)$ indicates that the charge carriers interact with an excitation spectrum that extends over a broad energy range. Blue line is at 100 K, red at 200 K. The dotted line is calculated for the simplest scattering model where the carriers are scattered at a constant rate $1/\tau_0$ of order $k_B T/\hbar$. The deviation from this model is pronounced at energies $\hbar\omega \gg k_B T$. Red arrow indicates an energy of $k_B \times 200$ K. (Adapted from ref. 7.) **b:** In Raman scattering, shown here for $YBa_2Cu_3O_7$, a broad electronic excitation spectrum is observed extending in energy up to 1 eV (8000 cm^{-1}) and beyond. The spectrum is featureless except for the sharp lines due to phonons. Blue curve is for 100 K, green for 300 K. At energies below $k_B T$ the spectrum decreases linearly to zero as ω tends to zero, and the inset shows that the slope is proportional to $1/T$ above T_c. (Adapted from ref. 8.) **Figure 4**

presence of a finite gap (see figure 5b).[14]

Several spectroscopic techniques have been employed to measure the magnitude and temperature-dependence of the superconducting gap $\Delta(T)$. They include electron tunneling with different arrangements between sample and counter electrode, high-resolution photoemission spectroscopy, optical spectroscopies and Raman scattering. In Raman spectroscopy below T_c, one observes that below a characteristic energy Δ, there is a reduction of the previously discussed broad electronic excitation spectrum, and also small changes of phonon frequencies and lifetimes. The result common to these studies of Δ is a $2\Delta/k_B T_c$ ratio that tends to be in the range 5 to 8, and hence larger than the weak-coupling BCS value of 3.5. (A few results, though, suggest values near 3–4.) There are also some hints that the gap may not be isotropic within the CuO_2 planes.

Two observations are not understood at this moment but are worth mentioning. One is that some of the spectroscopies reveal no sharp cut-off in the density of states below Δ, which would appear to be at odds with the temperature dependence of the superconducting order parameter ρ_s. The other observation is that the spectral features associated with Δ barely shift in energy when T_c is approached, almost as if the gap were nearly constant up to T_c.

Pairing mechanism

So far the pairing mechanism leading to T_c's above 100 K remains elusive, and it is impossible to capture all the pertinent arguments in a few paragraphs. The proposals range from conventional models (pairing mediated by various types of bosonic excitations), to exotic models based on quasiparticles in two dimensions that obey anyonic statistics (see the article by Philip Anderson and Robert Schrieffer on page 54). Experimental results in support of the exotic models remain inconclusive so far (see PHYSICS TODAY, February, page 17). The bosonic excitations in the conventional models may include:

▷ ordinary phonons or unusual lattice vibrations associated with the presumed anomalous polarizability of oxygen
▷ electronic excitations
▷ magnetic excitations.

The last two groups of excitations could be at energies higher than the phonons and thus could lead to higher T_c's.

Ideally one would want a theory that explains the various physical properties already observed and that identifies distinct, measurable features that are unique to a given pairing mechanism. Most of the models are not developed far enough to allow such detailed comparison with experiments. An exception is the conventional electron–phonon mechanism, which is well understood after decades of research, and many of the present discussions explore its applicability. The question is not whether there is an electron–lattice interaction, but if it is strong enough to produce the observed T_c's. The existence of an interaction between charge carriers and the crystal lattice in cuprates is indicated by results such as the increase of the phonon thermal conductivity below T_c, changes of phonon frequency and lifetime below T_c, and very subtle modifications of the local atomic coordination near T_c.

No direct measurement of the electron–phonon coupling strength exists so far. Knowing the phonon spectra from experiments led to wide agreement that strong coupling is required to get the high T_c's. Some researchers then take the large $2\Delta/k_B T_c$ ratio as indirect evidence for strong coupling. Others would point out, however, that the more directly measured density of electronic states and $\sigma(\omega,T)$ indicate only weak coupling—that is, λ less than about 0.4. It is also pointed out that large values of $2\Delta/k_B T_c$ are not necessarily indicative of strong coupling but could result from the large pair-breaking effects, which have been measured in $YBa_2Cu_3O_7$.

The discussion usually also includes the significance or insignificance of the isotope effect, which is found to be

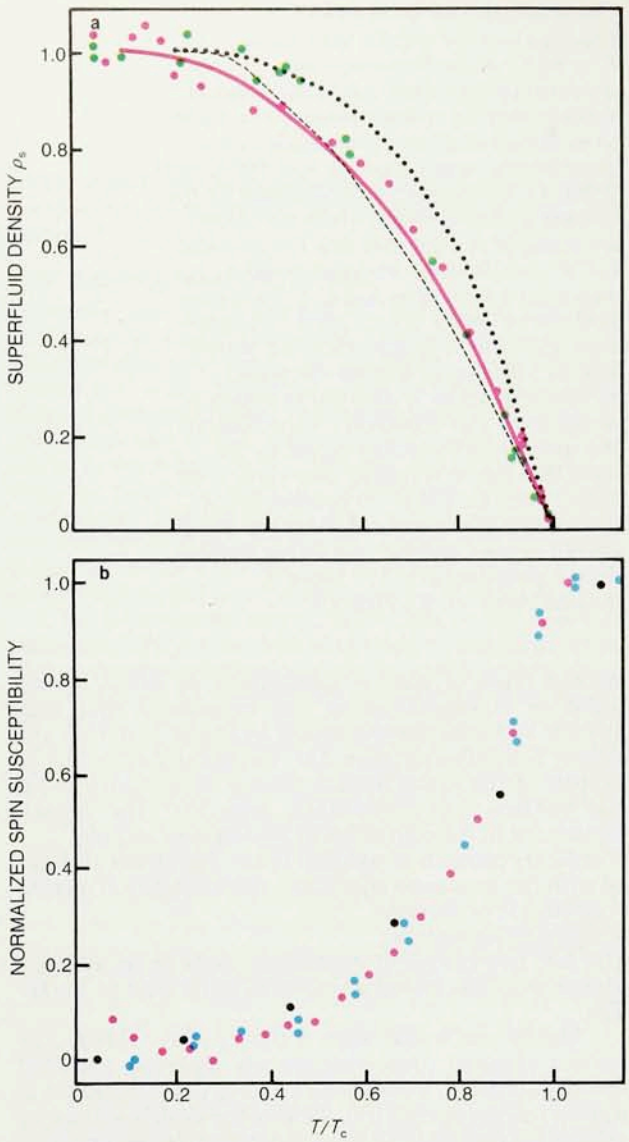

Existence of a nonzero gap over the entire Fermi surface is demonstrated by the flatness of these data at low T. **a:** The superfluid density, measured by $\rho_s = H_{c1}(T)/H_{c1}(0)$ (green data points) and by $\rho_s = \lambda^2(0)/\lambda^2(T)$ (red points and curve) in $YBa_2Cu_3O_7$. Weak-coupling BCS (dashed curve) and phenomenological two-fluid model (dotted curve) are also shown. (Adapted from ref. 13.) **b:** The spin susceptibility (nmr Knight shift) in $YBa_2Cu_3O_7$, measured on the O sites (blue), and measured on the Cu sites (red and black) by different groups. (Adapted from ref. 14.) **Figure 5**

small (or even zero) in materials with optimized T_c but can become sizable for compositions with non-optimized T_c. Alternative models are also proposed that involve, for instance, strong anharmonic lattice effects, but they are for the moment difficult to test experimentally.

This example illustrates the challenge for any theoretical idea: Over the past four years the diversity and quality of experimental data have grown to such a degree that the correct theory needs to explain consistently a large number of observed phenomena (only a few of which have been discussed here) in both the superconducting and the metallic states. Further progress will require a continuing interdisciplinary effort, involving a wide community of solid-state scientists to achieve the highest quality preparation of these complex materials and to apply skillfully the most advanced measurement techniques.

* * *

The author gratefully acknowledges the many collaborations and stimulating discussions he has had with colleagues at Bell Laboratories and elsewhere.

References

1. J. G. Bednorz, K. A. Müller, Z. Phys. B **64,** 189 (1986).
2. For up-to-date references and reviews of subfields, see Proc. 19th Int. Conf. on Low Temperature Phys. (LT 19), vols. I and II, Physica B **165** and **166** (1990); *Physical Properties of High Temperature Superconductors,* vols. I and II, D. M. Ginsberg, ed., World Scientific, Singapore (1989, 1990). *High Temperature Superconductivity,* Proc. Los Alamos Symp., 1989, K. S. Bedell, D. Coffey, D. E. Meltzer, D. Pines, J. R. Schrieffer, eds., Addison–Wesley, Redwood City, Calif. (1990). (The last book also contains a review by the author, with a more extensive list of references.)
3. R. J. Cava, Sci. Am., August 1990, p. 42.
4. Y. Tokura, H. Takagi, S. Uchida, Nature **337,** 345 (1989).
5. C. G. Olson, R. Liu, A. B. Yang, D. W. Lynch, A. J. Arko, R. S. List, B. W. Veal, Y. C. Chang, P. Z. Jiang, A. P. Paulikas, Science **245,** 731 (1989). G. Mante, R. Claessen, T. Buslaps, S. Harm, R. Manzke, M. Skibowski, J. Fink, Z. Phys. B **80,** 181 (1990).
6. S. Martin, A. T. Fiory, R. M. Fleming, L. F. Schneemeyer, J. V. Waszczak, Phys. Rev. Lett. **60,** 2194 (1988).
7. J. Orenstein, G. A. Thomas, A. J. Millis, S. L. Cooper, D. H. Rapkine, T. Timusk, L. F. Schneemeyer, J. V. Waszczak, Phys. Rev. B **42,** 6342 (1990). Z. Schlesinger, R. T. Collins, F. Holtzberg, C. Feild, S. H. Blanton, V. Welp, G. W. Crabtree, V. Fang, J. Z. Liu, Phys. Rev. Lett. **65,** 801 (1990). J. Schümann, W. Ose, J. Keller, K. F. Renk, B. Roas, L. Shultz, G. Saemann-Ischenko, Europhys. Lett. **8,** 679 (1989). K. Kamaras, S. L. Herr, C. D. Porter, N. Tache, D. B. Tanner, S. Etemad, T. Venkatesan, E. Chase, A. Juan, X. D. Wu, M. S. Hedge, B. Dutta, Phys. Rev. Lett. **64,** 84 (1990).
8. F. Slakey, M. V. Klein, J. P. Rice, D. M. Ginsberg, Phys. Rev. B **43,** 3764 (1991).
9. C. M. Varma, P. B. Littlewood, S. Schmitt-Rink, E. Abrahams, A. E. Ruckenstein, Phys. Rev. Lett. **63,** 1996 (1989).
10. T. Penney, S. von Molnar, D. Kaiser, F. Holtzberg, A. M. Kleinasser, Phys. Rev. B **38,** 2918 (1988). T. R. Chien, D. A. Brawner, Z. Z. Wang, N. P. Ong, Phys. Rev. B **43,** 6242 (1991).
11. D. Vaknin, S. K. Sinha, D. E. Moncton, D. C. Johnston, J. M. Newsam, C. R. Safinya, H. E. King, Jr., Phys. Rev. Lett. **58,** 2802 (1987).
12. See, for example, R. E. Walstedt, W. W. Warren, Science **248,** 1082 (1990).
13. See, for example, D. R. Harshman, G. Aeppli, E. J. Ansaldo, B. Batlogg, J. H. Brewer, J. F. Carolan, R. J. Cava, M. Celio, A. C. D. Chaklader, W. N. Hardy, S. R. Kreitzman, G. M. Luke, D. R. Noakes, M. Senba, Phys. Rev. B **36,** 2386 (1987); R. F. Kiefl, T. M. Riseman, G. Aeppli, E. J. Ansaldo, J. F. Carolan, R. J. Cava, W. N. Hardy, D. R. Harshman, N. Kaplan, J. R. Kempten, S. R. Kreitzman, G. M. Luke, B. X. Yang, D. L. Williams, Physica C **153–155,** 757 (1988); S. Anlage, B. W. Langley, G. Deutscher, R. W. Simon, J. M. Murduck, C.-B. Eom, M. R. Beasley, T. H. Geballe, in Proc. 19th Int. Conf. on Low Temperature Phys. (LT 19), vol. III, Physica B, in press; S. Sridhar, D.-H. Wu, W. Kennedy, Phys. Rev. Lett. **63,** 1873 (1989).
14. M. Takigawa, P. C. Hammel, R. H. Heffner, Z. Fisk, Phys. Rev. B **39,** 7371 (1989). S. E. Barret, D. J. Durand, C. H. Pennington, C. P. Slichter, T. A. Friedmann, J. P. Rice, D. M. Ginsberg, Phys. Rev. B **41,** 6283 (1990). ■